

Alkali Atoms Diffusion Mechanism in CuInSe_2 Explained by Kinetic Monte Carlo Simulations

Ramya Kormath Madam Raghupathy, Thomas D. Kühne, Graeme Henkelman, and Hossein Mirhosseini*

Adaptive kinetic Monte Carlo simulation (aKMC) is employed to study the dynamics and the diffusion of point defects in the CuInSe_2 lattice. The aKMC results show that lighter alkali atoms can diffuse into the CuInSe_2 grains, whereas the diffusion of heavier alkali atoms is limited to the Cu-poor region of the absorber. The key difference between the diffusion of lighter and heavier alkali elements is the energy barrier of the ion exchange between alkali interstitial atoms and Cu. For lighter alkali atoms like Na, the interstitial diffusion and the ion-exchange mechanism have comparable energy barriers. Therefore, Na interstitial atoms can diffuse into the grains and replace Cu atoms in the CuInSe_2 lattice. In contrast to Na, the ion-exchange mechanism occurs spontaneously for heavier alkali atoms like Rb and the further diffusion of these atoms depends on the availability of Cu vacancies. The outdiffusion of alkali substitutional atoms from the grains results in the formation of Cu vacancies which in turn increases the hole concentration in the absorber. In this respect, Na is more efficient than Rb due to the higher concentration of Na substitutional defects in the CuInSe_2 grains.

1. Introduction

The beneficial effects of alkali metal (AM) atoms on the performance of $\text{Cu}(\text{In}, \text{Ga})\text{Se}_2$ (CIGSe) based solar cells have been investigated for decades. It was observed that the presence of Na atoms in the CIGSe absorber enhances the p-type conductivity and open-circuit voltage.^[1–5] The effect of K atoms on the hole concentration was assumed to be similar to Na, although some studies showed the difference between K and Na effects on the cell performance.^[6] Heavier alkali elements like Rb and Cs were found to further enhance the conversion efficiency.^[7–12] Recently, the record-breaking efficiencies of 22.6% and 22.9% have been achieved for CIGSe solar cells with the Rb and Cs post-deposition treatment (PDT), respectively.^[13,14]

The presence of point defects in the CIGSe absorber material might lead to the formation of recombination centers and limit the device efficiency. Several experimental and theoretical efforts have been made to determine the role of point defects in the performance of solar cells. Experimentally, point defects in CuInSe_2 (CIGSe), CuGaSe_2 (CGSe), and CIGSe have been studied using different techniques such as photoluminescence,^[15–21] cathodoluminescence,^[22–24] and optical absorption measurement.^[25–27] Transient photocapacitance spectroscopy showed the presence of a deep defect level at about 0.8 eV above the valence band maximum in CIGSe films.^[28,29] In addition, deep-level transient spectroscopy probed at least two transition levels in the CIGSe absorber.^[30] These findings were supported by first-principles calculations.^[31–34]


Diffusion of constituent and external elements in the absorber layer were studied extensively as well. It was shown by *ab initio* calculations that Cu atoms are the most mobile atoms in CIGSe, whereas In atoms play no role in the mass transport.^[35–37] Moreover, first-principles results indicated that the diffusion of AM atoms in CIGSe depends on the AM atomic radii. The vacancy-mediated diffusion of Na has a larger migration barrier than those of K and Rb, whereas interstitial Na (Na_i) atoms diffuse faster than heavier AM in the interstitial site.^[34,38] It was found experimentally that Na diffusion in CIGSe is not controlled by Cu vacancies.^[39] In addition, the presence of Na atoms in the grain interior (GI) indicates the high mobility of Na atoms (Na interstitial diffusion).^[40] On the other hand, the concentration of K and Rb atoms in the GI is low despite the small migration barriers for

Dr. R. K. M. Raghupathy
Dynamics of Condensed Matter and Center
for Sustainable Systems Design
Chair of Theoretical Chemistry
University of Paderborn
Warburger Str. 100, D–33098 Paderborn, Germany

Prof. T. D. Kühne
Dynamics of Condensed Matter and Center
for Sustainable Systems Design
Chair of Theoretical Chemistry
University of Paderborn
Warburger Str. 100, D–33098 Paderborn, Germany

Prof. G. Henkelman
Department of Chemistry and the Institute for Computational
Engineering and Sciences
The University of Texas at Austin
Austin, TX 78712-0165, USA

Dr. H. Mirhosseini
Dynamics of Condensed Matter
and Center for Sustainable Systems Design
Chair of Theoretical Chemistry
University of Paderborn
Warburger Str. 100, D–33098 Paderborn, Germany
E-mail: mirhosse@mail.uni-paderborn.de

 The ORCID identification number(s) for the author(s) of this article can be found under <https://doi.org/10.1002/adts.201900036>

DOI: 10.1002/adts.201900036

the diffusion of the substitutional defects in the absorber layer.^[41] Experimental findings indicated that heavier AM atoms tend to segregate next to grain boundaries.^[40,42,43]

Several studies characterized the positive influences of AM atoms on the cell performance but the underlying reasons are still puzzling. It was suggested by Yuan et al.^[44] that the outdiffusion of Na and K atoms from the absorber layer could be the reason for the enhancement of hole concentration. So far, however, the majority of first-principles calculations were confined to static properties. To the best of our knowledge, the dynamics of the diffusion mechanisms for AM atoms in the CISE layer has not been investigated. Hence, in this work we studied the diffusion mechanisms of Cu and AM atoms in the CISE lattice by employing first-principles-based adaptive kinetic Monte Carlo (aKMC) simulations. Our results show that the key difference between the diffusion of lighter alkali metals (like Na) and heavier alkali metals (like Rb) is the energy barrier for the ion exchange between interstitial alkali atoms and Cu.

2. Experimental Section

To model the diffusion of atoms in the CISE lattice, first-principles-based adaptive KMC simulations were performed.^[45,46] The method is described as “adaptive” KMC because the list of possible events is calculated on the fly during the course of simulations. The reaction mechanisms and corresponding rates were calculated based on the harmonic transition state theory (hTST).^[47,48] The accurate characterization of saddle points on the potential energy surface can determine the most important dynamical events. The complete methodology details are described in ref. [45].

In this study, the simulations were performed on energy-minimized atomic configurations, where the impurities were initially placed on different lattice sites of CISE. In order to probe saddle points, the dimer method was used.^[49] The random saddle point searches initiated by displacing atoms with 5 Å distance from a central atom (either impurities in the CISE lattice or the interstitial atoms of the interest). For each local minimum the system visits, several searches were carried out to determine low-lying first-order saddle points. Once a saddle is found, the rate of the corresponding event is calculated as

$$k^{\text{hTST}} = \nu \cdot \exp\left(-\frac{\Delta E}{k_B T}\right) \quad (1)$$

where ν is the reaction prefactor and ΔE is the energy difference between the saddle point and the initial state. The reaction prefactors were calculated from the eigen-frequencies. In KMC simulations, all relevant kinetic events with low energy saddle points must be included in the rate table. For aKMC, where saddle points were found with the dimer method, searching for saddle points stops based on a dynamic stopping criterion. The confidence parameter (C) was used to evaluate the probability that an important saddle has not been missed from the history of previous saddle searches and it is defined as

$$C = \left(1 - \frac{1}{N_r}\right) \quad (2)$$

where N_r is the number of sequential searches that find relevant but redundant (nonunique) processes. The saddle point search was continued until the confidence level of 0.9 was achieved. After attaining this confidence level, the system evolved from the current stage to another one. The KMC algorithm proceeded the simulation to various states based on the information about the reaction mechanisms and associated rates provided in the event table. The time scales associated with the reaction mechanisms were found to be inversely proportional to their corresponding rates.

All calculations were performed within the framework of density functional theory (DFT) using the Vienna Ab-initio Software Package (VASP) software.^[50] The projector augmented (PAW) potentials used in the calculations were constructed such that the 3d¹⁰ 4s¹, 5s² 5p¹, and 4s² 4p⁴ shells were treated as valence states for Cu, In and Se, respectively. The calculations were carried out on a cubic 64-atom supercell. The Hubbard-corrected DFT calculations (with $U = 5.0$ eV on the Cu 3d electrons) were carried out using the projector augmented-wave method with a plane-wave cutoff of 350 eV.^[62,63] Atomic structures were considered to be relaxed when the residual force on each atom was less than 0.01 eV Å⁻¹. To determine the k -point mesh we did energy convergence test. Brillouin zone integration was performed with a $2 \times 2 \times 2$ Γ -centered k -point mesh with a density of 973 per atom.

The formation energy of a defect was calculated as

$$\begin{aligned} \Delta E_f = & E_{\text{tot}}(D, q) - E_{\text{tot}}(\text{bulk}) \\ & - \sum_i n_i (\mu_i^0 + \Delta\mu_i) \\ & + q [E_{\text{VBM}} + \mu_e + \Delta v_{0/b}] + E_{\text{corr}}^q \end{aligned} \quad (3)$$

where $E_{\text{tot}}(D, q)$ and $E_{\text{tot}}(\text{bulk})$ are the potential energies of supercells with the defect (D) in charge state q and the bulk supercell (without defects), respectively. The number of atoms of species i that are removed from/added to the system is indicated by n_i and μ_i^0 is the associated chemical potential of species i in the native elemental state. The thermodynamic limits of the chemical potentials were computed by determining the stability region for all the competing phases with respect to the reference structure. The thermodynamic limit of the chemical potential of species i is indicated by $\Delta\mu_i$. E_{VBM} is the valence band maximum of the bulk, μ_e is the Fermi energy level (electron chemical potential), which varies from 0 to the band gap of the system, and $\Delta v_{0/b}$ represents the correction term for the electrostatic alignment. E_{corr}^q represents the correction term for the total energy when the system is charged and is calculated by the approach proposed by Lany and Zunger.^[64]

3. Results and Discussion

The formation energies of point defects in CISE under Cu-poor and In-poor conditions^[37] are shown in **Table 1**. By comparing the formation energies, it is evident that Cu vacancy (V_{Cu}) and Cu interstitial (Cu_i) defects have the lowest formation energies among vacancy and interstitial defects, respectively. Regarding antisite defects, In_{Cu} is the most stable defect. We note that the two most

Table 1. Formation energies of intrinsic and AM-related defects in the most stable charge states. The formation energies are calculated when the Fermi level (electron chemical potential) is located at the valence band maximum.

Defect	Charge state	Formation energy [eV]	
		Cu poor	In poor
Cu _i	+1	0.9	0.6
V _{Cu}	-1	0.6	0.9
Cu _{In}	0	1.6	0.9
In _{Cu}	+2	-0.2	0.4
In _i	+3	2.2	2.5
V _{In}	+1	3.0	2.5
Se _i	+2	2.2	2.2
V _{Se}	0	2.2	2.2
Li _{Cu}	0	0.0	0.0
Na _{Cu}	0	0.4	0.5
K _{Cu}	0	1.4	1.5
Rb _{Cu}	0	1.9	2.3
Li _i	+1	0.6	0.3
Na _i	+1	1.0	0.8
K _i	+1	2.6	2.4

stable intrinsic defects in ClSe are donor defects and only V_{Cu} is an acceptor defect.^[31] That means that the formation of intrinsic defects in ClSe cannot increase the hole concentration. The formation of Cu_i could be hindered by growing films under Cu-poor conditions but this leads to the higher concentration of In_{Cu} defects that are harmful for p-type conductivity.^[30,51]

The formation of V_{Cu} and Cu_i defects in Cu-poor and In-poor ClSe have comparable formation energies. Hence, we have performed aKMC calculations for the systems containing these defects to investigate their diffusion mechanisms. Our results show that the migration barriers of these two defects are very different (see Table 2). The diffusion rates and occurrence of possible mechanisms for the Cu-related defects are shown in Figure 1a,b. The most frequent events in the system with Cu_i defects have

Table 2. Calculated migration barriers for Cu-related defects.

Diffusion mechanism	E _m [eV]
M ₁ : Cu _i → Cu _i	0.39
M ₂ : Cu _i → Cu _i	0.19
M ₃ : Cu _i → Cu _i	0.22
M ₄ : V _{Cu} → V _{Cu}	1.1
M ₅ : Cu → Cu _i	1.1

barriers smaller than 0.1 eV. Most of these events move the system back and forth to the states that are separated by low barriers (superbasin). The events that evolve the system to new states (M₁, M₂, and M₃) have the barriers of 0.39, 0.19, and 0.22 eV, respectively. These events are depicted in Figure 2a. A Cu_i atom with four Se nearest neighbors can jump to an interstitial site with three Se nearest neighbors. This process (M₁) has a migration barrier of 0.39 eV. The Cu atom can jump back and forth between two equivalent interstitial sites (with three Se nearest neighbors) with a low migration barrier of 0.19 eV (M₂). It is also possible that the Cu_i atom hops to a new interstitial site which is equivalent to the first interstitial position. This process (M₃) has a migration barrier of 0.22 eV.

While Cu_i atoms can move easily in the ClSe lattice, even at lower temperatures, the probability of a Cu atom jumping from a Cu lattice to a V_{Cu} site is relatively low. This event has an energy barrier comparable to the energy needed for a Cu atom to form a Cu_i defect (Figure 2b). The energy barrier for an In_{Cu} atom to jump to a V_{Cu} site is also about 1 eV (not shown here). That is, when a V_{Cu} site is present in the system, the probability of a Cu or In atom hopping from the Cu lattice into this vacancy site is low, even at higher temperatures.^[52] On the other hand, mobile Cu_i atoms can recombine with Cu vacancies. Cu_i defects are harmful for p-type conductivity and the process of Cu_i atoms hopping into V_{Cu} sites decreases the concentration of these donor-like defects. This process also reduces the concentration of Cu vacancies. Hence, the recombination process cannot improve the carrier mobility in ClSe. It also inhibits the fast diffusion of Cu_i atoms in ClSe.^[37]

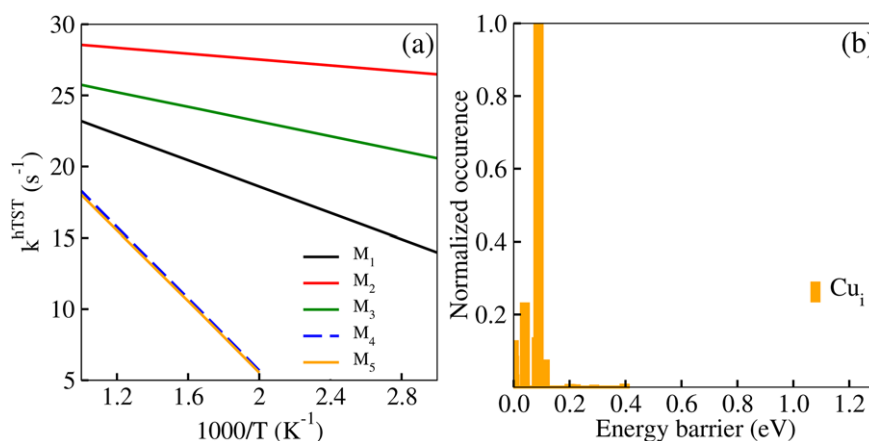


Figure 1. The a) rates and b) occurrences for the events that evolve the system with Cu-related defects.

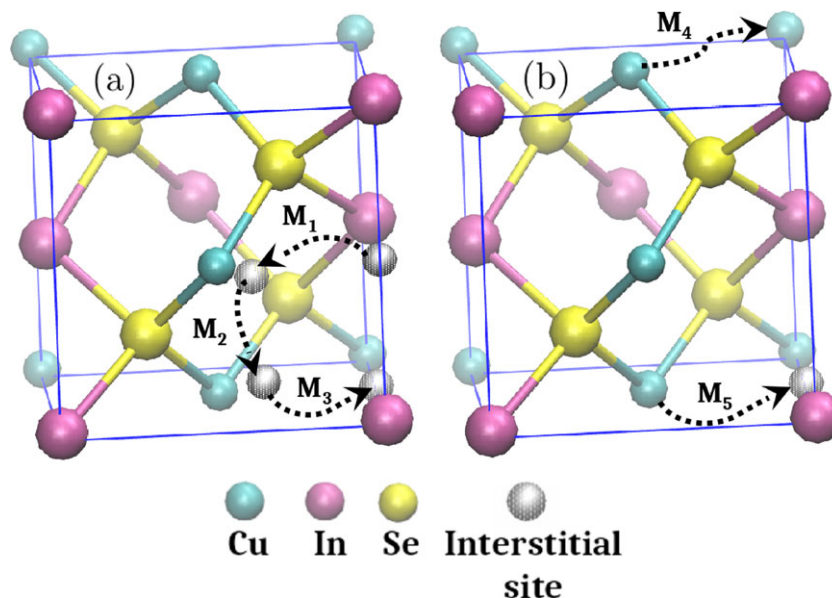


Figure 2. Migration paths for the events that evolve the system containing Cu defects.

It should be noted that some diffusion events with low migration barriers can occur only under certain conditions. For example, the ion exchange between an In interstitial (In_i) atom and a Cu atom in the Cu lattice has an energy barrier of 0.28 eV.^[53] Nevertheless, this event can only occur in the In-rich regions of the absorber, where the concentration of In_i defects is high. This ion-exchange mechanism leads to an even more Cu-depleted CISE layer by replacing Cu atoms with In atoms in the Cu lattice.^[54]

When AM atoms are introduced into the system, they can occupy different sites in the CISE lattice depending on their atomic radii (see Table 1). The formation energies indicate that lighter AM like Na can incorporate into CISE by forming substitutional and interstitial defects whereas, heavier alkali atoms like Rb can incorporate into CISE by replacing Cu in the CISE lattice. By comparing the defect formation energies, one expects a lower concentration of heavier alkali atoms in the CISE grains.

The enhancement of hole concentration after the AM-PDT cannot be explained by the formation of AM-related point defects. It has been argued that AM_{Cu} substitutional defects can reduce the concentration of In_{Cu} defects, which are detrimental to p-type conductivity.^[55,56] By comparing the formation energies of Na_{Cu} and In_{Cu} , one can conclude that replacing the latter with the former is possible only under very In-poor and Na-rich conditions. The formation of K_{Cu} or Rb_{Cu} instead of In_{Cu} is even less likely owing to the large differences between the formation energies. It has been proposed that the hole concentration in the absorber layer increases due to the formation of AM_{In} substitutional defects, which are acceptor defects.^[57] While these defects can introduce holes into the system, p-type conductivity cannot be improved owing to the formation of transition levels in the band gap. These deep transition levels are detrimental to p-type conductivity. Furthermore, the concentration of AM_{In} substitutional defects is relatively low owing to the large formation energy of

these defects.^[37] Experimental results also confirmed the absence of such acceptor levels in CISE and CGSe.^[58,59]

Similar to intrinsic defects, the formation of AM point defects cannot increase the hole concentration in the absorber layer. In contrast, these defects could be harmful for p-type conductivity. AM interstitial defects are positively charged and act as donor defects. In addition, AM atoms that occupy V_{Cu} sites reduce the concentration of V_{Cu} . It can be concluded that the formation of AM point defects in the CISE grains cannot explain the enhancement of hole concentration. The reason for the increase of hole concentration can be attributed to the diffusion of AM in the CISE lattice, as it is discussed below.

Some diffusion events in CISE and CGSe have been already studied with nudged elastic band (NEB) calculations.^[34,35,53] We note that the number of events that can be probed by the NEB method is limited since the diffusion paths are not known a priori and are required for each event. In contrast to NEB calculations, aKMC simulations can probe many different events for a given system. The process of finding new saddle points requires only specifying the initial atomic configuration. AKM simulations enhance the possibility for finding new mechanisms and their corresponding saddle points. In Table 3 we compare some similar diffusion events probed by aKMC and NEB.

Figure 3a and b show the rates and occurrences for the events that govern the diffusion of Na atoms in CISE. The migration barriers are listed in Table 4. It should be noted that two migration barriers for Na_i atoms are due to the nonequivalent interstitial sites of Na. The diffusion of Na atoms from the most stable interstitial site to the less stable site has a barrier that is 0.47 eV higher than the reversed mechanism. The diffusion barriers of Na atoms via interstitial and vacancy-mediated mechanisms are comparable. This means that both diffusion mechanisms are likely to happen in the Cu-poor region of CISE, for example, close to grain boundaries and CISE surfaces. In the region with the low

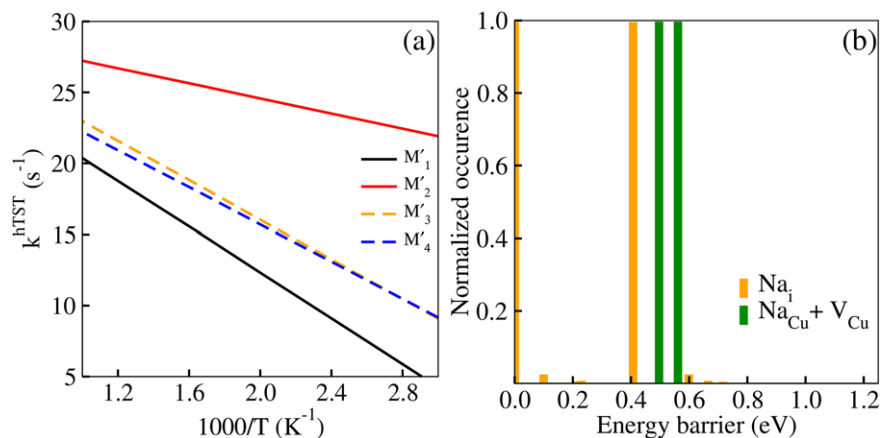


Figure 3. a) The rates and b) occurrences for the events that control the diffusion of Na defects.

concentration of Cu vacancies, however, the dominant mechanism is the interstitial diffusion. This mechanism is responsible for the diffusion of Na atoms into the GI, where the Cu-vacancy-mediated diffusion mechanism is hindered.

As we can see in Table 4, one of the possible events that evolves the system with Na_i defect is the ion exchange between Na_i and Cu atoms (M₃). This event occurs when a Na_i atom replaces a Cu atom in the Cu lattice and the Cu atom diffuses to the interstitial site as it is shown in **Figure 4**. After an ion exchange between Cu and Na_i occurs, the Cu_i atom can either jump back to the Cu lattice or diffuse in the CISE lattice, as it is shown in Figure 2a. Although the energy barrier for the former (0.10 eV) is lower than the latter (0.22 eV), our aKMC results show that both events are likely to happen at higher temperatures due to their low energy barriers. The ion-exchange mechanism is part of the mechanism that leads to the enhancement of the hole concentration in CISE, which is discussed later.

By increasing the size of AM atoms, the migration barrier associated with the diffusion of the AM interstitial atom increases.^[34] At the same time, the energy barrier for the AM-Cu ion exchange decreases. For Na, the diffusion of an interstitial atom has a comparable energy barrier (0.69 eV) to the Na–Cu ion exchange (0.59 eV), whereas the diffusion of a Rb_i atom has a larger migration barrier (1.2 eV) compared to the Rb-Cu ion-exchange mechanism (0 eV). That means that Rb_i atoms spontaneously replace the Cu atoms in the Cu lattice and the further diffusion of Rb atoms depends on the concentration of Cu vacancies. The differ-

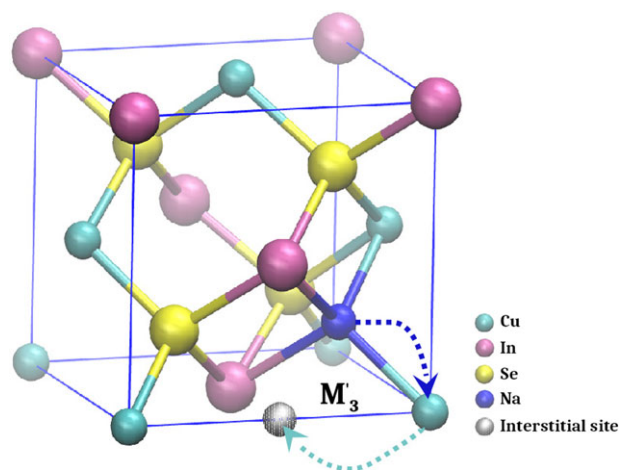


Figure 4. AM-Cu ion-exchange mechanism.

ences between the diffusion mechanisms of Na and Rb atoms can explain the higher concentration of Na atoms in the GI compared to Rb atoms.^[40] Rb atoms can mainly diffuse in the regions where the concentration of Cu vacancies is high, which is close to the surface or GBs. Experiments have shown that heavier AM atoms tend to segregate next to GBs rather than diffuse into the GI.^[40,42,43] Our formation energy calculations also showed the tendency of AM atoms to segregate close to GBs.^[60]

By decreasing the temperature, the solubility of external atoms in CISE decreases. At the same time the concentration of intrinsic defects also decreases. Since Cu_i atoms are very mobile in the system, they can diffuse out of the GI rapidly. AM atoms can also diffuse out from the GI. However, the diffusion of substitutional

Table 3. Energy barriers for the selected events calculated by NEB and akMC.

Process	NEB	akMC
Cu _i → Cu _i '	0.15	0.1–0.4
V _{Cu} → V _{Cu} '	1.1	1.1
Na _i → Na _i '	0.54 (0.37)	0.66 (0.22)
Li _{Cu} → Li _{Cu} '	0.70	0.76
Na _{Cu} → Na _{Cu} '	0.42	0.56
K _{Cu} → K _{Cu} '	0.25	0.47
Rb _{Cu} → Rb _{Cu} '	0.30	0.49

Table 4. Calculated migration barriers for Na-related defects.

Diffusion mechanism	E _m [eV]
M ₁ : Na _i → Na _i	0.69
M ₂ : Na _i → Na _i	0.22
M ₃ : Na _i → Cu _i + Na _{Cu}	0.59
M ₄ : Na _{Cu} + V _{Cu} → Na _{Cu} ' + V _{Cu} '	0.56

atoms depends mainly on the V_{Cu} concentration. The concentration of V_{Cu} in the GI is not sufficiently high to let the substitutional defects diffuse out of the GI as fast as Cu_i atoms. The energy barriers for Na and Rb substitutional atoms to become interstitial atoms are also very high, which make these processes unlikely. The outdiffusion of AM substitutional atoms should start from the Cu-poor regions of the absorber, for example the regions near GBs.

The vacancy-mediated outdiffusion of AM atoms from the GI leads to the enhancement of the Cu vacancy concentration in the GI and consequently the enhancement of the hole concentration in the absorber. In this regard, Na atoms are more efficient than Rb atoms. The effectiveness of the formation of V_{Cu} by the outdiffusion of AM atoms depends on the concentration of AM substitutional defects in the GI. In turn, the concentration of the AM substitutional defects in the GI depends on the AM-Cu ion-exchange mechanism. The concentration of Na atoms in the GI is higher than Rb owing to the facile diffusion of Na_i atoms into the GI followed by the ion exchange between Na_i and Cu atoms.

It should be noted that the formation of Cu vacancies can take place due to the rapid outdiffusion of Cu_i as compared to the outdiffusion of AM substitutional defects. Otherwise, the V_{Cu} sites will be occupied by Cu_i atoms. The outdiffusion of Na atoms can take place by diffusion of Na_i atoms out of the GI as well. However, the outdiffusion of Na_i does not lead to the formation of Cu vacancies. It is reported that the incorporation of a high percentage of Na atoms into CISE could be harmful for the cell efficiency.^[61] One possible reason for this observation could be the insufficient outdiffusion of Na_i atoms that are donor defects and harmful for p-type conductivity.

4. Conclusions

We have investigated the dynamics and migration barriers associated with the diffusion of alkali metals in the CISE lattice from aKMC simulations. From these simulations, it is evident that the diffusion of alkali atoms in the CISE lattice depends primarily on their atomic radii. While lighter AM interstitial atoms can diffuse into the GI, the vacancy-mediated diffusion of heavier AM atoms is limited to the Cu-poor regions of the absorber. In addition to the size of the AM atoms, the AM-Cu ion-exchange mechanism also plays a dominant role in the diffusion of AM atoms. If the AM-Cu ion-exchange mechanism has a lower energy barrier compared to the interstitial diffusion (like Rb), then the ion exchange occurs spontaneously and the further diffusion of AM atoms depends on the available V_{Cu} sites. In the case of Na, the interstitial diffusion and the ion-exchange mechanisms have comparable energy barriers. Therefore Na_i atoms can diffuse into the CISE grains and replace Cu atoms in the Cu lattice. This is the reason for the higher concentration of Na atoms in the GI in comparison to Rb atoms. The outdiffusion of AM atoms enhances the hole concentration in the absorber layer. In this aspect, Na is more efficient than heavier alkali atoms owing to higher concentration of Na substitutional defects in the grains. The positive effect of heavier AM atoms could be due to the passivation of GBs or improving the electronic structure of interfaces.^[60] This shows that the high efficiency of solar cell after the PDT could be due to the combined effect of both lighter and heavier AM atoms.

Acknowledgements

The authors would like to acknowledge financial support from the German *Bundesministerium für Wirtschaft und Energie (BMWi)* for the speedCIGS project (0324095C). The authors would like to acknowledge the Paderborn Center for Parallel Computing (PC²) for computing time on OCuLUS and FPGA-based supercomputer NOCTUA. The authors gratefully acknowledge the Gauss Centre for Supercomputing e.V. (<https://www.gauss-centre.eu>) for funding this project by providing computing time on the GCS Supercomputer SuperMUC at the Leibniz Supercomputing Centre (www.lrz.de).

Conflict of Interest

The authors declare no conflict of interest.

Keywords

adaptive kinetic Monte Carlo simulations, CuInSe_2 absorbers, diffusion mechanisms, migration barriers, thin-film solar cells

Received: February 18, 2019

Revised: March 22, 2019

Published online:

- [1] T. Nakada, D. Iga, H. Ohbo, A. Kunioka, *Jpn. J. Appl. Phys.* **1997**, *36*, 732.
- [2] D. Rudmann, A. F. da Cunha, M. Kaelin, F. Kurdesau, H. Zogg, A. N. Tiwari, G. Bilger, *Appl. Phys. Lett.* **2004**, *84*, 1129.
- [3] D. Rudmann, D. Brémaud, A. da Cunha, G. Bilger, A. Strohm, M. Kaelin, H. Zogg, A. N. Tiwari, *Thin Solid Films* **2005**, *480-481*, 55, EMRS 2004.
- [4] K. Granath, M. Bodegård, L. Stolt, *Sol. Energy Mater. Sol. Cells* **2000**, *60*, 279.
- [5] V. Probst, J. Rimmasch, W. Riedl, W. Stetter, J. Holz, H. Harms, F. Karg, H. W. Schock, in *Proceedings of 1994 IEEE 1st World Conference on Photovoltaic Energy Conversion - WCPEC (A Joint Conference of PVSC, PVSEC, and PSEC)* vol. 1, **1994**, pp. 144–147.
- [6] C. P. Muzzillo, *Sol. Energy Mater. Sol. Cells* **2017**, *172*, 18, and references therein.
- [7] A. Chirilă, P. Reinhard, F. Pianezzi, P. Bloesch, A. R. Uhl, C. Fella, L. Kranz, D. Keller, C. Gretener, H. Hagendorfer, D. Jaeger, R. Erni, S. Nishiwaki, S. Buecheler, A. N. Tiwari, *Nat. Mater.* **2013**, *12*, 1107.
- [8] P. Pistor, D. Greiner, C. A. Kaufmann, S. Brunken, M. Gorgoi, A. Steigert, W. Calvet, I. Lauermann, R. Klenk, T. Unold, M. -C. Lux-Steiner, *Appl. Phys. Lett.* **2014**, *105*, 063901.
- [9] E. Handick, P. Reinhard, J. -H. Alsmeyer, L. Köhler, F. Pianezzi, S. Krause, M. Gorgoi, E. Ikenaga, N. Koch, R. G. Wilks, S. Buecheler, A. N. Tiwari, M. Bär, *ACS Appl. Mater. Interfaces* **2015**, *7*, 27414.
- [10] E. Handick, P. Reinhard, R. G. Wilks, F. Pianezzi, T. Kunze, D. Kreikemeyer-Lorenzo, L. Weinhardt, M. Blum, W. Yang, M. Gorgoi, E. Ikenaga, D. Gerlach, S. Ueda, Y. Yamashita, T. Chikyow, C. Heske, S. Buecheler, A. N. Tiwari, M. Bär, *ACS Appl. Mater. Interfaces* **2017**, *9*, 3581.
- [11] E. Avancini, R. Carron, T. P. Weiss, C. Andres, M. Bürki, C. Schreiner, R. Figi, Y. E. Romanyuk, S. Buecheler, A. N. Tiwari, *Chem. Mater.* **2017**, *29*, 9695.
- [12] P. Jackson, D. Hariskos, R. Wuerz, O. Kiowski, A. Bauer, T. M. Friedlmeier, M. Powalla, *Phys. Status Solidi RRL* **9**, 28.
- [13] P. Jackson, R. Wuerz, D. Hariskos, E. Lotter, W. Witte, M. Powalla, *Phys. Status Solidi RRL* **10**, 583.

- [14] T. Kato, J. Wu, Y. Hirai, H. Sugimoto, V. Bermudez, *IEEE J. Photovoltaics* **2019**, *9*, 325–330.
- [15] P. Migliorato, J. L. Shay, H. M. Kasper, S. Wagner, *J. Appl. Phys.* **1975**, *46*, 1777.
- [16] P. W. Yu, *Solid State Commun.* **1976**, *18*, 395.
- [17] C. Rincón, J. González, G. Sánchez Pérez, *J. Appl. Phys.* **1983**, *54*, 6634.
- [18] G. Dagan, F. Abou-Elfotouh, D. J. Dunlavy, R. J. Matson, D. Cahen, *Chem. Mater.* **1990**, *2*, 286.
- [19] J. Stankiewicz, W. Giriat, J. Ramos, M. Vecchi, *Sol. Energy Mater.* **1979**, *1*, 369.
- [20] A. Bauknecht, S. Siebentritt, J. Albert, M. C. Lux-Steiner, *J. Appl. Phys.* **2001**, *89*, 4391.
- [21] S. Siebentritt, I. Beckers, T. Riemann, J. Christen, A. Hoffmann, M. Dworzak, *Appl. Phys. Lett.* **2005**, *86*, 091909.
- [22] G. Massé, N. Lahlou, N. Yamamoto, *J. Appl. Phys.* **1980**, *51*, 4981.
- [23] G. Massé, E. Redjai, *J. Appl. Phys.* **1984**, *56*, 1154.
- [24] G. Massé, K. Djessas, F. Guastavino, *J. Phys. Chem. Solids* **1991**, *52*, 999.
- [25] C. Rincón, J. González, *Phys. Status Solidi (b)* **1982**, *110*, K171–K174.
- [26] C. Rincón, C. Bellabarba, *Phys. Rev. B* **1986**, *33*, 7160.
- [27] C. Rincón, C. Bellabarba, J. González, G. S. Pérez, *Sol. Cells* **1986**, *16*, 335.
- [28] J. T. Heath, J. D. Cohen, W. N. Shafarman, D. X. Liao, A. A. Rockett, *Appl. Phys. Lett.* **2002**, *80*, 4540.
- [29] T. Sakurai, H. Uehigashi, M. Islam, T. Miyazaki, S. Ishizuka, K. Sakurai, A. Yamada, K. Matsubara, S. Niki, K. Akimoto, *Thin Solid Films* **2009**, *517*, 2403.
- [30] M. Igalson, M. Wimbor, J. Wennerberg, *Thin Solid Films* **2002**, *403–404*, 320.
- [31] S. B. Zhang, S. -H. Wei, A. Zunger, H. Katayama-Yoshida, *Phys. Rev. B* **1998**, *57*, 9642.
- [32] L. E. Oikkonen, M. G. Ganchenkova, A. P. Seitsonen, R. M. Nieminen, *J. Appl. Phys.* **2013**, *114*, 083503.
- [33] E. Ghorbani, J. Kiss, H. Mirhosseini, G. Roma, M. Schmidt, J. Windeln, T. D. Kühne, C. Felser, *J. Phys. Chem. C* **2015**, *119*, 25197.
- [34] M. Malitckaya, H. -P. Komsa, V. Havu, M. J. Puska, *J. Phys. Chem. C* **2017**, *121*, 15516.
- [35] L. E. Oikkonen, M. G. Ganchenkova, A. P. Seitsonen, R. M. Nieminen, *J. Appl. Phys.* **2013**, *113*, 133510.
- [36] J. Pohl, K. Albe, *J. Appl. Phys.* **2010**, *108*, 023509.
- [37] J. Pohl, A. Klein, K. Albe, *Phys. Rev. B* **2011**, *84*, 121201.
- [38] T. Maeda, A. Kawabata, T. Wada, *Japanese J. Appl. Phys.* **2015**, *54*, 08KC20.
- [39] R. V. Forest, B. E. McCandless, X. He, A. A. Rockett, E. Eser, K. D. Dobson, R. W. Birkmire, *J. Appl. Phys.* **2017**, *121*, 245102.
- [40] A. Vilalta-Clemente, M. Raghuvanshi, S. Duguay, C. Castro, E. Cadel, P. Pareige, P. Jackson, R. Wuerz, D. Hariskos, W. Witte, *Appl. Phys. Lett.* **2018**, *112*, 103105.
- [41] R. Wuerz, W. Hempel, P. Jackson, *J. Appl. Phys.* **2018**, *124*, 165305.
- [42] P. Schöppe, S. Schönherr, P. Jackson, R. Wuerz, W. Wisniewski, M. Ritzer, M. Zapf, A. Johannes, C. Schnohr, C. Ronning, *ACS Appl. Mater. Interfaces* **2018**, *10*, 40592.
- [43] A. Stokes, M. Al-Jassim, D. Diercks, A. Clarke, B. Gorman, *Sci. Rep.* **2017**, *7*, 14163.
- [44] Z. -K. Yuan, S. Chen, Y. Xie, J. -S. Park, H. Xiang, X. -G. Gong, S. -H. Wei, *Adv. Energy Mater.* **6**, 1601191.
- [45] G. Henkelman, H. Jónsson, *J. Chem. Phys.* **2001**, *115*, 9657.
- [46] L. Xu, G. Henkelman, *J. Chem. Phys.* **2008**, *129*, 114104.
- [47] C. Wert, C. Zener, *Phys. Rev.* **1949**, *76*, 1169.
- [48] G. H. Vineyard, *J. Phys. Chem. Solids* **1957**, *3*, 121.
- [49] G. Henkelman, H. Jónsson, *J. Chem. Phys.* **1999**, *111*, 7010.
- [50] G. Kresse, J. Furthmüller, *Comput. Mater. Sci.* **1996**, *6*, 15.
- [51] M. Igalson, P. Zabierowski, *Thin Solid Films* **2000**, *361–362*, 371.
- [52] O. Lundberg, J. Lu, A. Rockett, M. Edoff, L. Stolt, *J. Phys. Chem. Solids* **2003**, *64*, 1499.
- [53] L. E. Oikkonen, M. G. Ganchenkova, A. P. Seitsonen, R. M. Nieminen, *J. Phys.: Condens. Matter* **2014**, *26*, 345501.
- [54] D. Liao, A. Rockett, *Appl. Phys. Lett.* **2003**, *82*, 2829.
- [55] M. A. Contreras, B. Egaas, P. Dippo, J. Webb, J. Granata, K. Ramanathan, S. Asher, A. Swartzlander, R. Noufi, Conference Record of the Twenty Sixth IEEE Photovoltaic Specialists Conference - 1997, **1997**, pp. 359.
- [56] S. -H. Wei, S. B. Zhang, A. Zunger, *J. Appl. Phys.* **1999**, *85*, 7214.
- [57] D. W. Niles, K. Ramanathan, F. Hasoon, R. Noufi, B. J. Tielsch, J. E. Fulghum, *J. Vac. Sci. Technol., A* **1997**, *15*, 3044.
- [58] D. J. Schroeder, A. A. Rockett, *J. Appl. Phys.* **1997**, *82*, 4982.
- [59] S. Schuler, S. Siebentritt, S. Nishiwaki, N. Rega, J. Beckmann, S. Brehme, M. C. Lux-Steiner, *Phys. Rev. B* **2004**, *69*, 045210.
- [60] M. Chugh, T. D. Kühne, H. Mirhosseini, *ACS Appl. Mater. Interfaces* <https://org.doi.10.1021/acsami.9b02158>
- [61] J. E. Granata, J. R. Sites, S. Asher, R. J. Matson, Conference Record of the Twenty Sixth IEEE Photovoltaic Specialists Conference - 1997, **1997**, pp. 387.
- [62] P. Blöchl, *Phys. Rev. B* **1994**, *50*, 17953.
- [63] V. I. Anisimov, J. Zaanen, O. K. Andersen, *Phys. Rev. B* **1991**, *44*, 943.
- [64] S. Lany, A. Zunger, *Phys. Rev. B* **2008**, *78*, 235104.